

# FAD-modified SiO<sub>2</sub>/ZrO<sub>2</sub>/C ceramic electrode for electrocatalytic reduction of bromate and iodate

Eduardo Marafon · Lauro T. Kubota · Yoshitaka Gushikem

Received: 31 March 2008 / Accepted: 11 April 2008 / Published online: 15 May 2008  
© Springer-Verlag 2008

**Abstract** SiO<sub>2</sub>/ZrO<sub>2</sub>/C carbon ceramic material with composition (in wt%) SiO<sub>2</sub>=50, ZrO<sub>2</sub>=20, and C=30 was prepared by the sol–gel-processing method. A high-resolution transmission electron microscopy image showed that ZrO<sub>2</sub> and the graphite particles are well dispersed inside the matrix. The electrical conductivity obtained for the pressed disks of the material was 18 S cm<sup>-1</sup>, indicating that C particles are also well interconnected inside the solid. An electrode modified with flavin adenine dinucleotide (FAD) prepared by immersing the solid SiO<sub>2</sub>/ZrO<sub>2</sub>/C, molded as a pressed disk, inside a FAD solution (1.0 × 10<sup>-3</sup> mol L<sup>-1</sup>) was used to investigate the electrocatalytic reduction of bromate and iodate. The reduction of both ions occurred at a peak potential of -0.41 V vs. the saturated calomel reference electrode. The linear response range (lrr) and detection limit (dl) were: BrO<sub>3</sub><sup>-</sup>, lrr=4.98 × 10<sup>-5</sup>–1.23 × 10<sup>-3</sup> mol L<sup>-1</sup> and dl=2.33 μmol L<sup>-1</sup>; IO<sub>3</sub><sup>-</sup>, lrr=4.98 × 10<sup>-5</sup> up to 2.42 × 10<sup>-3</sup> and dl=1.46 μmol L<sup>-1</sup> for iodate.

**Keywords** SiO<sub>2</sub>/ZrO<sub>2</sub>/C ceramic electrode · Electrical conductive ceramic · Flavin adenine dinucleotide · Electrochemical detection of bromate and iodate · Electrochemical sensor

## Introduction

Materials obtained by the sol–gel-processing method to construct electrochemical devices have attracted great interest over the past decades due to their remarkable facilities of obtaining homogenous electrochemical studies and applications [1–4]. Growing interest has been focused

on sol–gel-derived carbon ceramic electrodes (CCEs), which are generally prepared by incorporating graphite powder into a silicate gel matrix [5, 6]. The advantages presented by CCE, such as low cost, high stability, good surface-renewable repeatability, and easy preparation and modifying, have proportionate many efforts devoted to the preparation of modified CCE with different electroactive species for electroanalytical applications [7–14].

Flavoproteins play an important biological role in the electron transfer reactions in living systems, primarily due to the presence of flavin adenine dinucleotide (FAD). Other members of the flavin family include flavin mononucleotide, riboflavin (vitamin B<sub>2</sub>), and lumiflavin [15, 16]. FAD in particular has been extensively studied on several solid electrodes such as Au [17–19], Pt [20], glassy carbon [21–23], and titanium oxide-modified electrodes [24, 25].

Disinfection of drinking water by chlorine sometimes forms carcinogenic trihalomethanes, and therefore, recently, ozone has been alternatively used for the treatment. However, the bromate ion can be generated during the ozone treatment, if the water source contains bromide ion [26–28]. This powerful oxidant is a genotoxic carcinogen [29, 30].

Table salt is iodized with potassium iodate or iodine in most countries. The iodized salt is recognized as the method of choice and the most successful strategy for preventing iodide deficiency disorders [31]. Otherwise, an excess of iodine or iodate can produce goiter and hypothyroidism as well as hyperthyroidism [32].

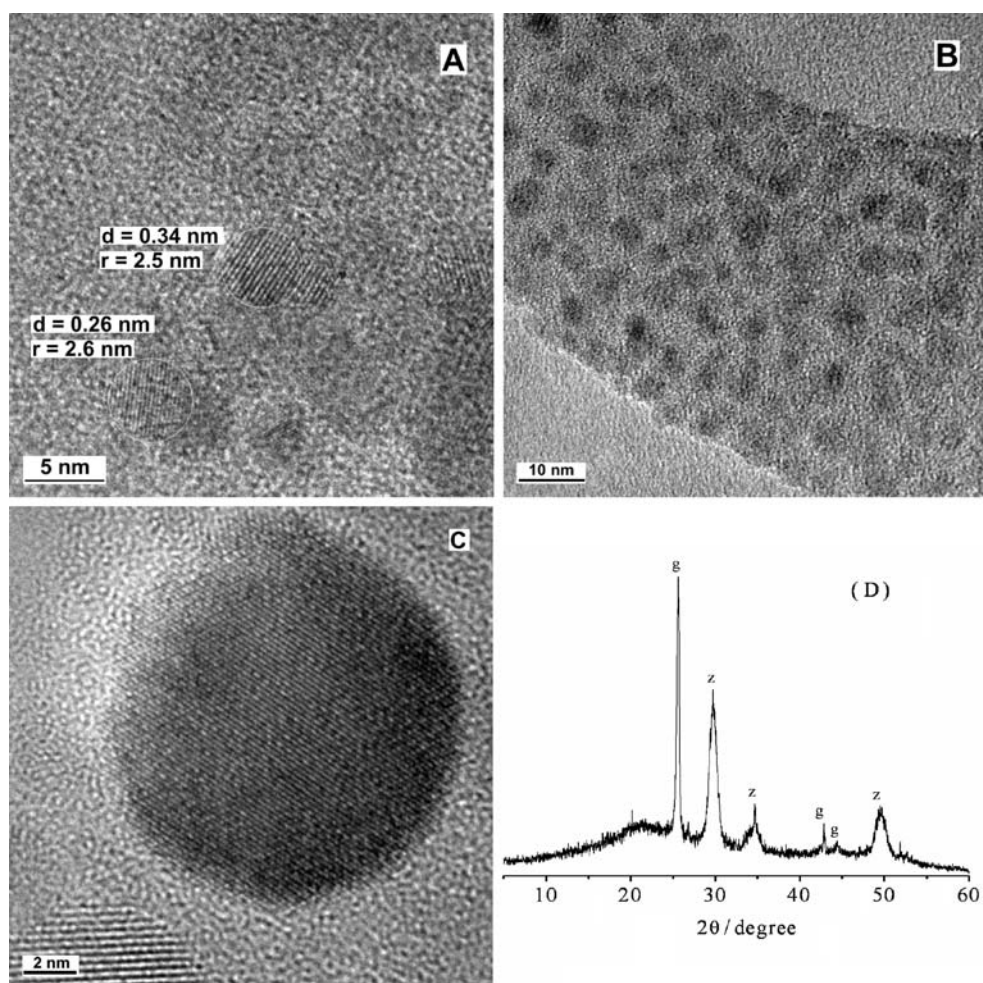
## Materials and methods

### Preparation of SiO<sub>2</sub>/ZrO<sub>2</sub>/C

The SiO<sub>2</sub>/ZrO<sub>2</sub>/C composite material, hereafter designated as SZC, was prepared by the sol–gel method according to a

E. Marafon · L. T. Kubota · Y. Gushikem (✉)  
Instituto de Química, Universidade Estadual de Campinas,  
P. O. Box 6154, 13084-971 Campinas, SP, Brazil  
e-mail: gushikem@iqm.unicamp.br

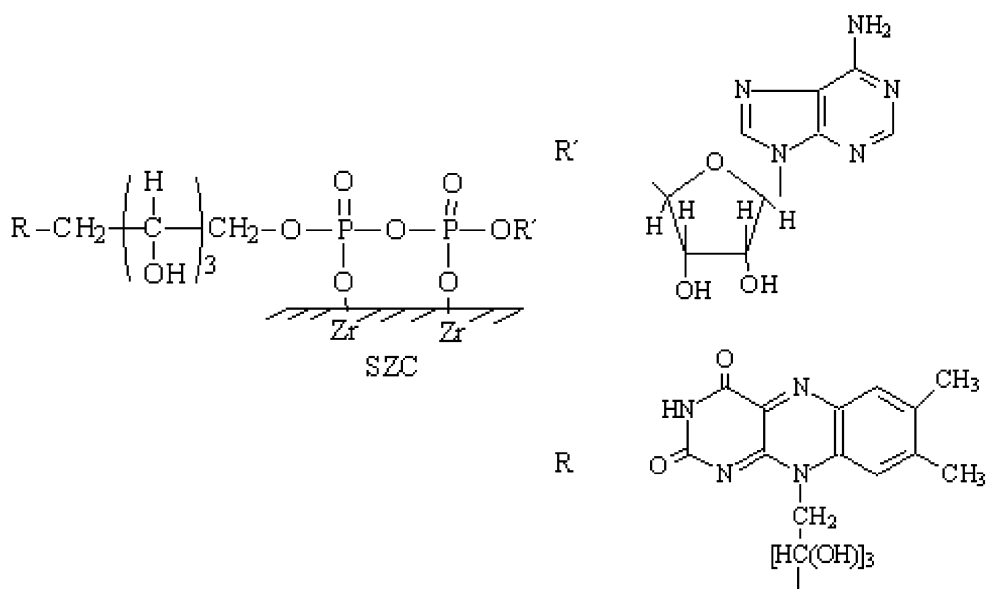
**Fig. 1** **a** HRTEM image for SZC heated at 343 K. **b** Image obtained by mass contrast for SZC heat treated at 1,273 K. **c** HRTEM of  $ZrO_2$  heat treated at 1,273 K. **d** The X-ray diffraction patterns obtained for sample heat treated at 1,273 K



previously described procedure [33]. In a solution of tetraethyl orthosilicate (TEOS; Aldrich) in pure ethanol in a 1:1 (v/v) proportion, an aqueous acid solution was added,

and the mixture was stirred for few hours at room temperature. An appropriate amount of zirconium tetrabutoxide (Aldrich) and graphite (Fluka) were added to the prehy-

**Fig. 2** Schematic representation of FAD immobilized on the SZC surface



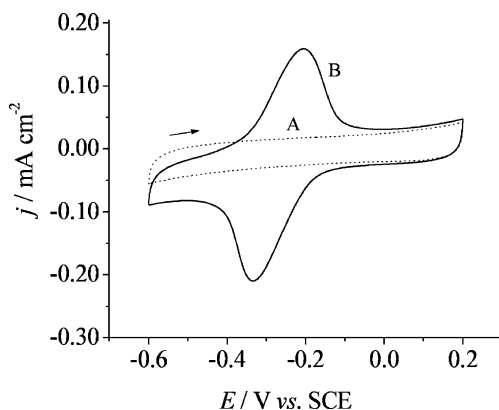


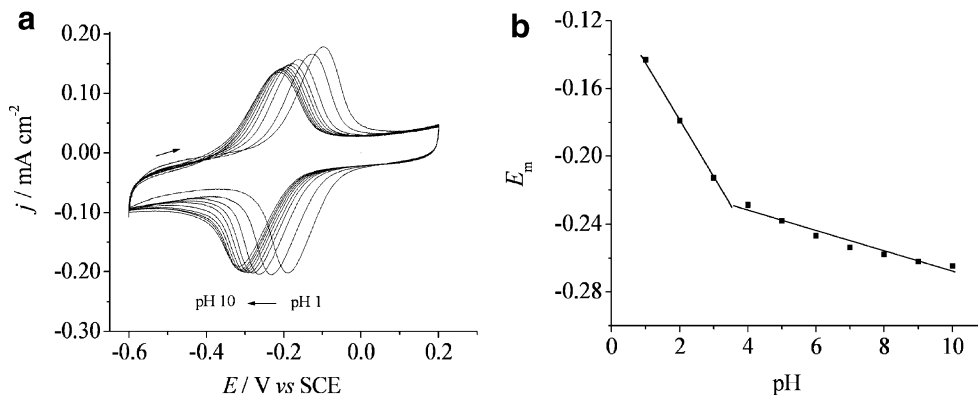
**Fig. 3** Cyclic voltammograms obtained for: **a** bare SZC electrode and **b** on SZC/FAD electrode, in 0.1 mol L<sup>-1</sup> KCl solution, pH 4, at a sweep rate of 5 mV s<sup>-1</sup>

drolyzed TEOS solution, followed by an additional small amount of the aqueous acid solution. The mixture was stirred and allowed to rest. The solvent was evaporated until gelation, and the obtained xerogel was ground to a fine powder. It was exhaustively washed with bidistilled water and ethanol and, finally, dried under vacuum.

**Preparation of the SZC carbon ceramic electrode and modification with FAD**

About 12 mg of the dried and powdered SZC was pressed at a pressure of 2.5 × 10<sup>3</sup> kg cm<sup>-2</sup> in a disk format. The pressed disk presenting an 8-mm diameter was glued at the end of a glass tube with the same external diameter and 15 cm length. The electrical contact was made by a copper wire, and pure graphite powder paste was inserted inside the glass tube [34]. The electrode modification was achieved by immersing the electrode into a 1.0 × 10<sup>-3</sup>-mol L<sup>-1</sup> FAD solution for 15 h. The FAD phosphate group reacts and adheres to the SZC surface resulting in a surface-modified electrode. The electrode surface is rinsed with deionized water before using.

**Fig. 4 a** Variation of  $E_m$  of SZC/FAD as a function of solution pH, obtained in 0.1 mol L<sup>-1</sup> KCl solution at a sweep rate of 5 mV s<sup>-1</sup>. **b** Plot of  $E_m$  vs. solution pH



*Transmission electron microscopy*

Images of high-resolution transmission electron microscopy (HRTEM) were obtained on a JEOL JEM-3010 with 0.17-nm resolution, operating with a voltage of 300 kV. The fine-powdered SZC material was dispersed in isopropyl alcohol and submitted to an ultrasound bath during 10 min, and the suspension was deposited on a copper grid, previously coated with a thin film of carbon (approximate thickness of 3 nm).

*Electrochemical measurements*

Electrochemical measurements were carried out with a conventional three-electrode electrochemical cell. A platinum wire acted as the counter electrode, and the working electrode was a SZC CCE. All the potentials were measured and referred to the saturated calomel reference electrode (SCE). The cyclic voltammograms of the adsorbed FAD were recorded, usually between -0.6 and +0.2 V in 0.1 mol L<sup>-1</sup> KCl solution free of oxygen. The solution pH was adjusted by adding HCl or NaOH solution. Amperometric measurements were performed by applying a fixed potential of -0.410 V. Finally, bromate and iodate anions in the appropriate concentration were added to detect them by voltammetry and amperometry.

**Results and discussions**

*Characteristics of the material*

To obtain information about the degree of dispersion of ZrO<sub>2</sub> particles in the SZC matrix, it was necessary to heat at 1,273 K under a nitrogen atmosphere to observe the crystalline ZrO<sub>2</sub> phase. For as-prepared samples, ZrO<sub>2</sub> is amorphous and therefore unobservable by the HRTEM technique.

Figure 1a shows the HRTEM image for SZC heated at 343 K under vacuum (0.13 Pa), and the observed fringes at

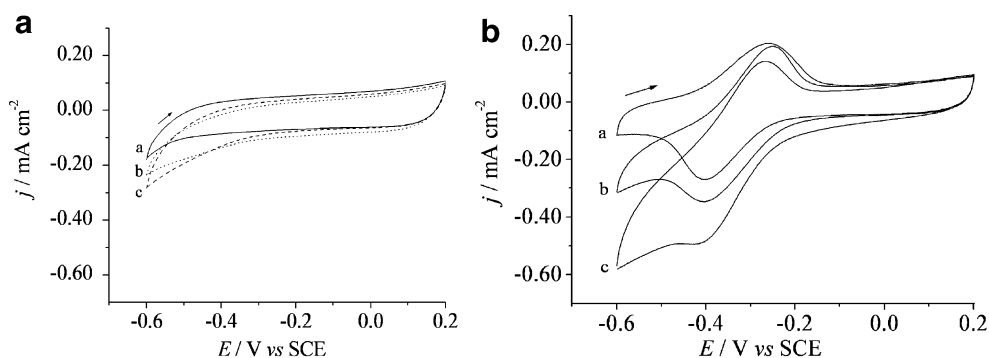


**Fig. 5 a** Cyclic voltammograms obtained with SZC electrode. *a* Immersed in the solution in absence of analyte; *b* solution containing  $[\text{BrO}_3^-]=5 \times 10^{-3} \text{ mol L}^{-1}$ ; *c* solution containing  $[\text{IO}_3^-]=5 \times 10^{-3} \text{ mol L}^{-1}$ . **b** Cyclic voltammograms obtained with SZC/FAD electrode: *a*

immersed in the solution in absence of analyte, *b* solution containing  $[\text{BrO}_3^-]=5 \times 10^{-3} \text{ mol L}^{-1}$ , *c* solution containing  $[\text{IO}_3^-]=5 \times 10^{-3} \text{ mol L}^{-1}$ . In **a** and **b**: solution of KCl 0.1 mol L<sup>-1</sup>, pH 4.0, and a scan rate of 10 mV s<sup>-1</sup>

0.26 and 0.34 nm of the nanoparticles in the micrograph are due to the crystalline phase of graphite [35]. According to the X-ray diffraction pattern (figure not shown), these two distances correspond to the (002) and (101) planes, respectively. For this sample, the HRTEM presented in Fig. 1b shows the image obtained by mass contrast, where ZrO<sub>2</sub> appears as darker particles, in comparison to the graphite, which is more transparent. In Fig. 1c, for the sample heated at 1,273 K, both ZrO<sub>2</sub> and graphite crystalline particles are clearly observed, where the larger one corresponds to the ZrO<sub>2</sub> phase. SiO<sub>2</sub> remained as an amorphous phase. The X-ray diffraction patterns obtained from this heated material is shown in Fig. 1d where peaks marked ( $2\theta$  in degree, [hkl]) with *g* (graphite) and *z* (ZrO<sub>2</sub>) refers to: (a) *g*=25.8 [002], 42.2 [100], 44.5 [101]; (b) *z*=30.0 [101], 34.8 [002], 49.7 [002].

According to these data, it is noted that ZrO<sub>2</sub> particles are highly dispersed in the SZC matrix. The active centers are the ZrOH groups present on the surface of the matrix (heated at 343 K), and they are the responsible to link with the phosphate groups of FAD through the P–O–Zr bond.

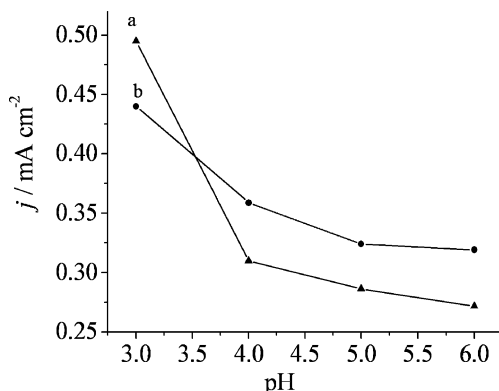


**Fig. 6** Cathodic peak current for SZC/FAD in presence of  $5.0 \times 10^{-3} \text{ mol L}^{-1}$  of **a**  $\text{IO}_3^-$  and **b**  $\text{BrO}_3^-$  obtained in 0.1 mol L<sup>-1</sup> KCl solution at solutions' pH between 3.0 and 6.0 and scan rate of 10 mV s<sup>-1</sup>

## Electrochemistry

The electrical conductivity of the material SZC was obtained following a procedure previously described [34]. The obtained pressed disk presented a conductivity of 18 S cm<sup>-1</sup>, and then it was used to prepare the electrode as described above in the experimental part. After that, it was immersed in a FAD solution. Since this compound possesses phosphate groups, which normally have good affinity for the ZrOH groups, present on the SZC pressed disk surface, an efficient immobilization of the FAD on the electrode surface could be obtained [35]. The immobilization of this species may occur through the Z–O–P linkage, as shown in Fig. 2:

Figure 3 shows the cyclic voltammogram obtained with SZC and SZC/FAD electrodes in the solution saturated with argon. In contrast to the unmodified CCE, clear anodic and cathodic peaks were registered for the FAD-modified CCE. A well-defined redox couple with a midpoint potential of  $E_m = -0.270 \text{ V vs. SCE}$  ( $E_m = (E_{pa} + E_{pc})/2$ ), where  $E_{pa}$  and  $E_{pc}$  are the anodic and cathodic peak potentials, respec-

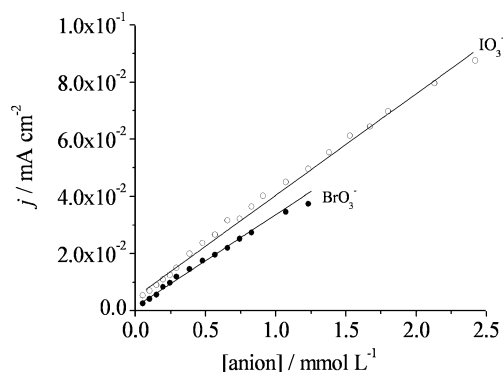


**Fig. 7** Plot of current densities against concentration of bromate and iodate, obtained by chronoamperometry on SZC/FAD-modified CCE. Applied potential of  $-0.41 \text{ V}$  and solution pH 4.0

**Table 1** Analytical parameters of SZC/FAD electrode for detection of  $\text{BrO}_3^-$  and  $\text{IO}_3^-$  at pH 4.0

Analyte	Linear response range, $\text{mol L}^{-1}$	$r^2$ ( $n$ )	Detection limit, $\mu\text{mol L}^{-1}$
$\text{BrO}_3^-$	$4.98 \times 10^{-5}$ – $1.23 \times 10^{-3}$	0.997 (14)	2.33
$\text{IO}_3^-$	$4.98 \times 10^{-5}$ – $2.42 \times 10^{-3}$	0.998 (21)	1.46

tively, is observed for the SZC/FAD-modified electrode. This value is similar to those found for FAD adsorbed on  $\text{TiO}_2$ -modified carbon fibers [24] and silica gel-modified zirconium oxide [36]. No decrease in the peak current was observed after many repeated cycles, suggesting that FAD is strongly adsorbed on the SZC electrode surface. The surface concentration of electroactive species  $\Gamma_c$  was estimated to be  $2.21 \times 10^{-8} \text{ mol cm}^{-2}$  by the following equation [37].

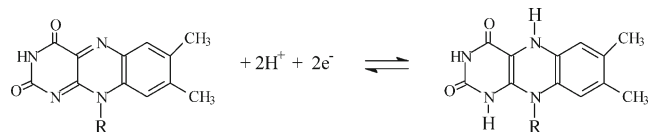
$$Q = nFA\Gamma_c$$

where  $Q$  is the background-corrected charge obtained by integrating the area under the anodic peak,  $A$  is the electrode geometric surface area, and the other symbols have their usual meaning. It should be pointed out that the calculated surface coverage is an effective attribute (per cross-section of the electrode) and does not reflect the real number of FAD molecules per surface area of the exposed zirconium oxide.

The variation of  $E_m$  with the solution pH showed to be dependent between 1 and 4, while between pH 4 and 10,  $E_m$  becomes virtually independent of pH (Fig. 4).

This is not expected because it is supported that in the redox process of flavins, two protons and one or two electrons are involved [38–40]. These dependences are quite different from the electroactivity of flavins in solution: 60 mV/pH for  $6.5 \geq \text{pH} \geq 10.5$  and 30 mV/pH in the range of

pH between 6.5 and 10.5 [41]. The first inflection point is attributed to the  $\text{p}K_a$  for the deprotonation of N-1 of the reduced flavin (the fully reduced hydroquinone form), and the second inflection point is due to the  $\text{p}K_a$  for the deprotonation of the oxidized isoalloxazine ring N-5 (the oxidized quinone form) [41], which has been explained by the FAD redox reaction:



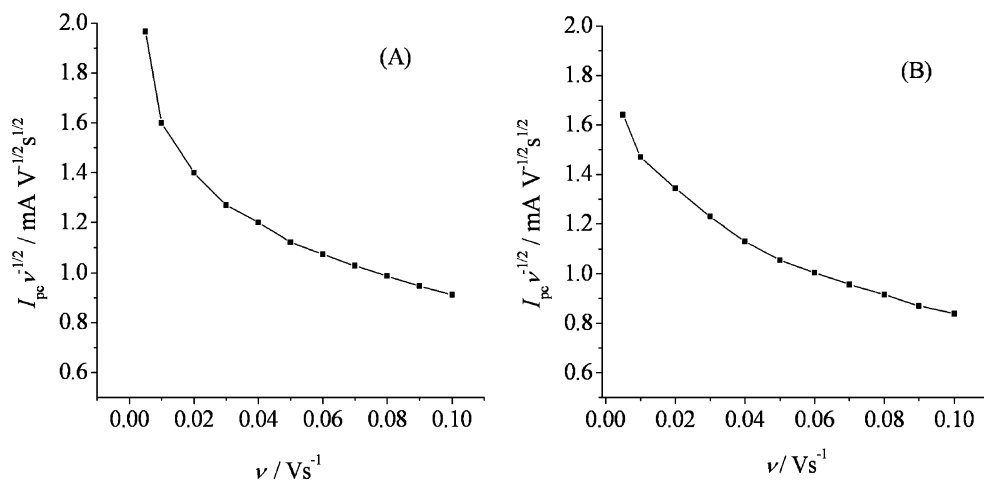
### The electrocatalytical reduction of bromate and iodate by SZC/FAD-modified electrode

To evaluate the electrocatalytic activity of the SZC CCE modified with FAD toward bromate and iodate reduction, cyclic voltammograms were obtained in the absence (Fig. 5a) and presence of these species (Fig. 5b). A cathodic peak current is observed at  $-0.410 \text{ V vs. SCE}$ . These results demonstrated that the SZC/FAD-modified electrode electrocatalytically reduces  $\text{BrO}_3^-$  and  $\text{IO}_3^-$  in an aqueous solution (Fig. 5b).

The results presented above show that the SZC/FAD-modified CCE in acidic solutions had an electrocatalytic reduction activity for  $\text{BrO}_3^-$  and  $\text{IO}_3^-$  that was pronounced directly through the redox couple occurring at a potential of  $-0.41 \text{ V vs. SCE}$ .

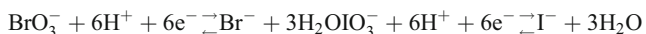
As both anions are strong oxidants at acidic conditions, the effect of pH on the potential of  $\text{BrO}_3^-$  and  $\text{IO}_3^-$  reduction was examined over the pH range between 3 and 6. A decrease in the reduction current density for  $\text{BrO}_3^-$  and  $\text{IO}_3^-$  is observed as the solutions' pH increase from 3.0 up to 6.0 (Fig. 6).

**Fig. 8** Variation of the scan rate-normalized current ( $I_p/\nu^{1/2}$ ) with a scan rate on the SZC/FAD-modified electrode in solution containing  $5.0 \times 10^{-3} \text{ mol L}^{-1}$  bromate (a) and iodate (b). The experiments were performed in  $0.1 \text{ mol L}^{-1}$  KCl solution at pH 4.0





The reduction of both anions in acidic solutions can occur according to the reactions:



The chronoamperometric behavior of the SZC/FAD electrode was examined in the presence of bromate and iodate. The response time of the SZC/FAD-modified electrode was very fast for  $\text{BrO}_3^-$  and  $\text{IO}_3^-$ , i.e., about 0.5 s (figure not shown), and presented a straight line with correlation factors  $r^2=0.997$  and 0.998, respectively (Fig. 7).

The results obtained from amperometric measurements are summarized in Table 1. This behavior shows that the SZC/FAD-modified CCE is a useful amperometric sensor for the determination of bromate and iodate.

Additional information about bromate and iodate reduction on the modified electrode surface was obtained by analyzing the catalytic current from the cyclic voltammograms. According to Andrieux and Sev ant [42], a theoretical model for the catalytic current  $I_p$  depends on the potential scan rates  $\nu$  as follows:

$$I_p = 0.496FAC_o^*D^{1/2}(F\nu/RT)^{1/2}$$

where  $C_o^*$  is the substrate concentration,  $D$  represents the diffusion coefficient of the substrate,  $F$  is the Faraday constant, and  $R$  and  $T$  are the gas constant and temperature, respectively. Furthermore, a catalytic system behaves as a totally irreversible system controlled by diffusion for large values of kinetic parameters (i.e., high value of the catalytic rate constant,  $k$ ) [42, 43]. First, a plot of the catalytic current  $I_p$  vs. the square root of the potential scan rate,  $\nu^{1/2}$ , was plotted (figure not shown) suggesting that the process is controlled by mass transport. However, a deviation from the linearity for higher scan rates is clearly verified, suggesting a kinetic limitation. Second, a plot of the sweep rate-normalized current  $I_p/\nu^{1/2}$  vs. the sweep rate (Fig. 8) exhibited the characteristic shape of the  $\text{EC}_{\text{cat}}$  process for bromate and iodate. The profiles of the curves (B) and (C) show that the catalytic current are still present in higher scan rates, suggesting good reaction rates between immobilized FAD and bromate and iodate. It is also clearly observed that the reduction reaction rate for iodate is about three times faster than that observed for bromate in the present system.

## Conclusions

The SZC electrode was modified by immersing into a FAD solution and resulted in SZC/FAD, where the chemical species is bonded to the surface through Zr–O–P bonding.

Furthermore, this electrode was used for the electrocatalytic reduction of bromate and iodate. The reduction reactions occurred at a cathodic peak potential of  $-0.41$  V vs. SCE, and changes of the solutions' pH between 3.0 and 6.0 showed a decrease in substantial current densities for higher values of pH. The reduction current densities for bromate and iodate, at a fixed pH of 4.0, were linearly dependent over a wide range of concentrations. These studies indicated that the SZC/FAD-modified electrode can be used as an amperometric sensor for  $\text{BrO}_3^-$  and  $\text{IO}_3^-$ .

**Acknowledgments** EM is indebted to FAPESP for fellowship (grant 04/00919-5) and YG and LTK for financial support (grant 00/11103-5).

## References

1. Wang B, Li B, Wang Z, Xu G, Wang Q, Dong S (1999) *Anal Chem* 71:1935
2. Salimi A, Pourbeyram S (2003) *Talanta* 60:205
3. Walcarius A (2001) *Electroanalysis* 13:701
4. Wang J (1999) *Anal Chim Acta* 399:21
5. Tsionsky M, Gun J, Glezer V, Lev O (1994) *Anal Chem* 66:1747
6. Rabinovich L, Lev O (2001) *Electroanalysis* 13:265
7. Wang P, Wang X, Zhu G (2000) *Electrochim Acta* 46:637
8. Wang P, Wang X, Zhu G (2000) *Electroanalysis* 12:1493
9. Shankaran DR, Uehara N, Kato T (2002) *Sens Actuators B Chem* 87:442
10. Shankaran DR, Uehara N, Kato T (2003) *Biosens Bioelectron* 18:721
11. Salimi A, Pourbeyram S, Haddadzadeh H (2003) *J Electroanal Chem* 542:39
12. Salimi A, Abdi K, Khayatiyan G (2004) *Electrochim Acta* 49:413
13. Niedziolka J, Opallo M (2003) *Electrochem Commun* 5:924
14. Opallo M, Sazek-Maj M, Shul G, Hayman CM, Page PCB, Marken F (2005) *Electrochim Acta* 50:1711
15. Akimoto M, Sato Y, Okubo T, Todo H, Hasegawa T, Sugibayashi K (2006) *Biol Pharm Bull* 29:1779
16. Massey V (2000) *Biochem Soc Trans* 28:283
17. Ksenzhek SO, Petrova SA (1983) *J Electroanal Chem* 11:105
18. Noll G, Kozma E, Grandori R, Carey J, Schodl T, Hauska G, Daub J (2006) *Langmuir* 22:2378
19. Wang Y, Zhu G, Wang E (1997) *Anal Chim Acta* 338:97
20. Gorton L, Johansson G (1980) *J Electroanal Chem* 113:151
21. Verhagen MFJM, Hagen WR (1992) *J Electroanal Chem* 334:339
22. Ivnova YN, Karyakin AA (2004) *Electrochem Commun* 6:120
23. Karyakin AA, Ivanova YN, Revunova KV, Karyakina EE (2004) *Anal Chem* 76:2004
24. Kubota LT, Gorton L, Roddick-Lanzilotta A, McQuillan AJ (1998) *Bioelectrochem Bioenerg* 47:39
25. Milsom EV, Perrott HR, Peter LM, Marken F (2005) *Langmuir* 21:9482
26. Takayanagi T, Makamoto I, Mbuna J, Driouich R, Motomizu S (2006) *J Chromatogr A* 1128:298
27. Kruithof JC, Meijers RT (1995) *Water Suppl* 117:13
28. Xie L, Shang C (2007) *Chemosphere* 66:1652
29. Kurokawa Y, Maekawa A, Takahashi M, Hayashi Y (1990) *Environ Health Perspect* 87:309
30. Kurata Y, Diwan BA, Ward JM (1992) *Food Chem Toxicol* 30:965
31. Jakmunee J, Grudpan K (2001) *Anal Chim Acta* 428:299

32. Salimi A, Noorbakhsh A, Ghadermarzi M (2007) *Sens Actuators B* 123:530
33. Marafon E, Francisco MSP, Lucho AMS, Landers R, Gushikem Y (2005) Brazilian Patent Br PI 0506395-7
34. Marafon E, Lucho AMS, Francisco MSP, Landers R, Gushikem Y (2006) *J Braz Chem Soc* 17:1605
35. Alfaya AAS, Gushikem Y, de Castro SC (2000) *Microp Mesopor Mater* 39:57
36. Yamashita M, Rosatto SS, Kubota LT (2002) *J Braz Chem Soc* 13:635
37. Wang J (1994) *Analytical electrochemistry*. VCH, New York, p 170
38. Gorton L, Johansson G (1980) *Electroanal Chem* 113:151
39. Bergel A, Comtat M (1991) *J Electroanal Chem* 302:219
40. Honeychurch MJ, Ridd MJ (1996) *Electroanalysis* 8:362
41. Ksenzhek OS, Petrova SA (1983) *Bioelectrochem Bioenerg* 11:105
42. Andrieux CP, Savéant JM (1978) *J Electroanal Chem* 93:163
43. Bard AJ, Faulkner LR (2001) *Electrochemical methods fundamentals and applications*, 2nd edn. Wiley, New York